Malaya Journal of Matematik, Vol. 8, No. 3, 845-851, 2020

https://doi.org/10.26637/MJM0803/0019

# Marangoni convection in superposed fluid and anisotropic porous layers with throughflow

Y. H. Gangadharaiah[1*], K. Ananda[2] and H. Nagarathnamma[3]

**Abstract**

Marangoni convective flow of fluid layer overlying a porous layer with anisotropic permeability and thermal diffusivity is addressed. Flow analysis has been carried out in presence of throughflow. Beavers–Joseph's slip condition is applied to the fluid-porous layer interface. The boundaries are known to be rigid, but permeable, and insulated to fluctuations in temperature. The problem of own value resulting from the stability analysis is solved through regular perturbation technique. Flow pattern with the influence of pertinent parameters namely the throughflow parameter, mechanical, thermal anisotropy parameters Prandtl number and depth ratio is investigated. Expression of critical Marangoni number is computed and analyzed. It is found that the depth of the relative layers, the direction of throughflow and mechanical and thermal anisotropy parameters deeply affect system stability. Reducing the parameter of mechanical anisotropy and increasing the parameter of thermal anisotropy contributes to process stabilization. In addition, the probability of regulating surface driven convection is discussed in detail through the appropriate choice of physical parameters.

**Keywords**

Composite layer, Mechanical anisotropy, Thermal anisotropy, Throughflow.

**AMS Subject Classification**

35Q30.

[1] *Department of Mathematics, Sir M. Visvesvaraya Institute of Technology, Bangalore-562157, India.*
[2] *Department of Mathematics, New Horizon College of Engineering, Bangalore-560 103, India.*
[3] *Department of Mathematics, Dr. Ambedkar Institute Of Technology, Bangalore-560056, India.*
*__Corresponding author__: [1] gangu.honnappa@gmail.com

**Article History**: Received **02** March **2020**; Accepted **19** May **2020**



## Contents



## 1. Introduction

The problem of Convective flows heat and species transport at the interface between a fluid and a porous region is encountered in a wide range of industrial and geophysical applications, such as cooling of electronic system, flows in fuel cells, thermal hydraulics of nuclear reactor, chemical processing equipment, filtration methods, the extraction of oil from underground reservoirs, contamination of groundwater, manufacture of composite materials and the flow of biological materials and so on (Vafai [1]; Nield and Bejan [2]; Nield and Bejan [3]). Marangoni flows most frequently occur when localized deposition of a surface tensioning agent such as a surfactant allows a gradient of surface tension to build (for examples, see references (Grotberg and Gaver [4–6] and Afsar-Siddiqui et al. [7]. This gradient induces an outward stream of convective Marangoni from the deposition area. Induced Marangoni flow can be used to enhance drug delivery in patients with obstructive pulmonary conditions such as cystic fibrosis lung disease, where accumulation of dehydrated mucus affects airway aerodynamics and subsequent patterns of aerosol deposition in the lung (for examples, see references Grotberg [8] Halpern et al. [9] and Bertram and Gaver [10]. Chen [11] has implemented a linear stability analysis of convective instability in composite layers with a vertical throughflow for isothermal boundaries. It is noticed that both stabilizing and destabilizing influences due to vertical flow can be improved in such a physical configuration, So, the driven instability is possible in either a fluid or a porous layer. Khalili et al. [12] investigated the effect of throughflow in superimposed fluid and porous layers on thermal convective instability with temperature disturbance isolated boundaries and a theoretical expression is obtained for the critical number of Rayleigh Sums et al. [13] investigated the effects of the throughflow on the porous layer over which over which lies a layer of fluid, while Shivakumara et al. [14] considered the effect of internal heating on the problem.

The problem that we want to look into is one of surface driven convection in a system consisting of a anisotropic porous layer underlying a fluid layer where there is throughflow in the system. The effects of throughflow in a two layer system is an potential method of regulating the onset of convection may be essential for industrial application. In order to be able to control convection, it is essential to determine when the convection is set in. In addition, to regulate the convective mechanisms in science, manufacturing, geophysics ,Medical field etc. the theory of throughflow is essential. The study of Marangoni convection with throughflow, however, is very limited. Shivakumara et al. [15] found an effective solution to the convection of Marangoni with throughflow and various boundary conditions. The Prandtl number and temperature boundary conditions have been found to play a major role in the destabilization that a small amount of throughflow. S. Saravanan and Sivakumar [16] have analyzed exact solution of Marangoni convection in a binary fluid with throughflow and Soret effect and shows that the Soret effect is seen only when the throughflow is weak. A non-zero mass flux through a liquid system is referred to as a throughflow through fluid injection at one boundary and fluid suction at another boundary. The possibility of controlling convective instability by adjusting the throughflow is of interest. This finds its application in the method of Czochralski, which is commonly used to produce large quantities of crystals grown in pure space. In this paper, therefore, we analyze the throughflow effects on system consisting of a anisotropic porous layer underlying a fluid layer by linear stability analysis and evaluated for the parameter of the throughflow and the factor anisotropy parameter discussed in detail.

## 2. Conceptual Model

The system under investigation consisting of an fluid layer of thickness $d$ (zone1) and saturating an underlying porous layer of thickness $d_m$ (zone2) with throughflow of constant vertical velocity $W_0$. Thus the $z$ indicating distances vertically

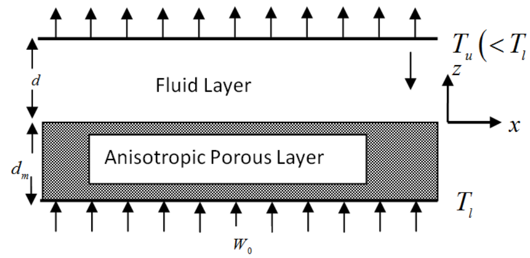


**Figure 1.** Physical configuration

upwards. The fluid-porous interface at $z = 0$.

## 3. Mathematical Formulation

The fluid-porous layers governing equations are:

**Zone1: Governing model for the layer of fluid** $(0 \leq z \leq d)$

$$\nabla \cdot \vec{V} = 0$$

$$\rho_0 \left[ \frac{\partial \vec{V}}{\partial t} + \left( \vec{V} \cdot \nabla \right) \vec{V} \right] = -\nabla p + \mu \nabla^2 \vec{V}$$

$$\frac{\partial T}{\partial t} \left( \vec{V} \cdot \nabla \right) T = \kappa \nabla^2 T$$

**Zone2: Governing model for the porous layer** $(-d_m \leq z \leq 0)$

$$\nabla \cdot \vec{V_m} = 0$$

$$\frac{\rho_0}{\phi} \frac{\partial \vec{V_m}}{\partial t} = -\nabla p_m - \mu \underset{\sim}{K}^{-1} \cdot \vec{V_m}$$

$$A \frac{\partial T_m}{\partial t} \left( \vec{V_m} \cdot \nabla_m \right) T_m = \nabla \cdot \{ \underset{\sim}{\kappa_m} \cdot \nabla T_m \}$$

In these equations, $T$ is the temperature, $\vec{V}$ the velocity vector, $p$ is the pressure, $\kappa$ is the thermal diffusivity, $\rho_0$ is the reference fluid density, The subscript $m$ refers to the value of the parameter in the zone2, while $\underset{\sim}{K}$ and $\underset{\sim}{\kappa_m}$ are respectively the tensors of permeability and effective thermal diffusivity which are given by

$$\underset{\sim}{K} = K_h(\hat{i}\hat{i} + \hat{j}\hat{j}) + K_v \hat{k}\hat{k}$$

$$\underset{\sim}{\kappa_m} = \kappa_{mh}(\hat{i}\hat{i} + \hat{j}\hat{j}) + \kappa_{mv} \hat{k}\hat{k}$$

where the subscripts $h$ and $v$ refer to the quantities in the horizontal and vertical directions respectively.

## 4. Linear Stability Analysis

The temperature distributions in the basic state is specified by

$$T_b(z) = T_0 - (T_0 - T_u) \left( \frac{1 - e^{W_0 z/\kappa}}{e^{W_0 d/\kappa} - 1} \right), 0 \leq z \leq d$$

$$T_{mb}(z_m) = T_0 + (T_1 - T_0)\left(\frac{1-e^{W_0 z_m/\kappa_{mv}}}{e^{-W_0 d_m/\kappa_{mv}}-1}\right), -d_m \le z_m \le 0,$$

Where $T_0$ is the interface temperature. The basic state is quiescent and is of the following form

$$\begin{aligned}(u,v,w,p,T) &= [0,0,W_0,p_b(z),T_b(z)]\\ (u_m,v_m,w_m,p_m,T_m) &= [0,0,W_0,p_{mb}(z),T_{mb}(z)].\end{aligned}$$

Infinitesimal disturbances are superimposed in the form of an investigation into the stability of the basic state $\vec{V} = \vec{V}'$, $T = T_b(z) + \theta$, $p = p_b(z) + p'$, $\vec{V_m} = \vec{V_m}'$ and $T_m = T_{mb}(z_m) + \theta_m$, $p_m = p_{mb}(z_m) + p'_m$.

Following the standard linear stability analysis procedure, we arrive at the following stability equations (see Chen et al. [11] and Shivakumara et al. [17] for details):

$$(D^2-a^2)(D^2-\eta D-a^2)W = 0 \tag{4.1}$$

$$(D^2-PeD-a^2)\ominus = \left[\frac{Pee^{Pea}}{1-e^{Pe}}\right]W \tag{4.2}$$

$$\left(\frac{1}{\xi}D_m^2-a_m^2\right)W_m = 0 \tag{4.3}$$

$$(D_m^2-Pe_mD_m-\chi a_m^2)\ominus_m = \left[\frac{Pe_me^{Pe_mz_m}}{1-e^{Pe_m}}\right]W_m \tag{4.4}$$

Here, $Pr = \nu/\kappa$ is the Prandtl number and $Pe = W_0 d/\kappa$ is the Peclet number. The corresponding quantities for the porous region are $Pr_m = \nu/\kappa_{mv} = Pr\varepsilon_T$, $Pe_m = W_0 d_m/\kappa_{mv} = Pe(\varepsilon_T/\zeta)$. Further, $Da = K_v/d_m^2$ is the Darcy number, $\chi = \kappa_{mh}/\kappa_{mv}$, $\xi = K_h/K_v$ are the thermal and mechanical anisotropy parameters, $\varepsilon_T = \kappa/\kappa_{mv}$ is the ratio of thermal diffusivity and $\eta = Pe/Pr$ is a non dimensional group. The boundary conditions are:

$$W = D\ominus = D^2W + Ma^2\theta = 0 \quad at\ z = 1 \tag{4.5}$$

$$W_m = D_m\ominus_m = 0 \quad at\ z_m = -1. \tag{4.6}$$

At the interface (i.e., $z = 0$) the continuity of velocity, temperature, heat flux, normal stress and the Beavers and Joseph [18] slip conditions are imposed. Accordingly, the conditions are:

$$W = \frac{\zeta}{\varepsilon_T}W_m, \ominus = \frac{\varepsilon_T}{\zeta}\ominus_m, D\ominus = D_m\ominus_m \tag{4.7}$$

$$\left[D^2-\eta D-3a^2\right]DW = \frac{-\zeta^4}{\varepsilon_T Da\xi}D_mW_m \tag{4.8}$$

$$\left[D^2-\frac{\beta\zeta}{\sqrt{Da\xi}}D\right]W = \frac{-\beta\zeta^3}{\varepsilon_T\sqrt{Da\xi}}D_mW_m \tag{4.9}$$

where, $\zeta = d/d_m$ is the ratio of fluid layer to porous layer thickness.

## 5. Analytical Solution

Equations (4.1)-(4.4) can be solved analytically using regular perturbation technique, subjected to boundary conditions, (4.5)-(4.9). The variables are expressed in terms of the small wave number to study the validity.

$$(W,\ominus) = \sum_{i=0}^{N}(a^2)^i(W_i,\ominus_m) \tag{5.1}$$

$$(W_m,\ominus_m) = \sum_{i=0}^{N}\left(\frac{a^2}{\zeta^2}\right)^i(W_{mi},\ominus_{mi}) \tag{5.2}$$

Substitution of equations (5.1) and (5.2) into equations (4.1)-(4.4) and the boundary conditions (4.5)-(4.9) yields a sequence of equations for the unknown functions $W_i(z)$, $\ominus_i(z)$, $W_{mi}(z_m)$ and $\ominus_{mi}(z_m)$ for $i = 0,1,2,3,\ldots$. At the leading order in $a^2$ equations (4.1)-(4.4) become respectively,

$$D^4W_0 - \eta D^3W_0 = 0 \tag{5.3}$$

$$D^2\ominus_0 - PeD\ominus_0 = W_0 f(z) \tag{5.4}$$

$$D_m^2W_{m0} = 0 \tag{5.5}$$

$$D_m^2\ominus_{m0} - Pe_mD_m\ominus_{m0} = W_{m0}g(z_m) \tag{5.6}$$

where

$$\begin{aligned}f(z) &= \frac{Pe}{1-e^{Pe}}e^{Pez}\\ g(z_m) &= \frac{Pe_m}{e^{Pe_m}-1}e^{Pe_mz_m}\end{aligned}$$

and the equations (4.5)-(4.9) become

$$\begin{aligned}W_0 &= 0,\ D\ominus_0 = 0,\ DW_0 = 0 \quad at\ z = 1\\ W_{m0} &= 0,\ D_m\ominus_{m0} = 0 \quad at\ z_m = -1.\end{aligned}$$

And at the interface(i.e $z = 0$)

$$W_0 = \frac{\zeta}{\varepsilon_T}W_{m0},\ \ominus_0 = \frac{\varepsilon_T}{\zeta}\ominus_{m0},\ D\ominus_0 = D_m\ominus_{m0}$$

$$D^3W_0 - \eta D^2W_0 = \frac{-\zeta^4}{\varepsilon_T Da\xi}D_mW_{m0}$$

$$D^2W_0 - \frac{\beta\zeta}{\sqrt{Da\xi}}DW_0 = \frac{-\beta\zeta^3}{\varepsilon_T\sqrt{Da\xi}}D_mW_{m0}$$

The solution to the zeroth order equations (5.3)-(5.6) is given by

$$W_0 = 0,\ \ominus_0 = \frac{\varepsilon_T}{\zeta},\ W_{n0} = 0,\ \ominus_{m0} = 1.$$

At the first order in $a^2$ equations (4.1)-(4.4) then reduce to

$$D^4W_1 - \eta D^3W_1 = 0 \tag{5.7}$$

$$D^2\ominus_1 - PeD\ominus_1 = W_1 f(z) + \frac{\varepsilon_T}{\zeta} \tag{5.8}$$

$$D_m^2W_{m1} = 0 \tag{5.9}$$

$$D_m^2\ominus_{m1} - Pe_mD_m\ominus_{m1} = W_{m1}g(z_m) + \chi \tag{5.10}$$

and the equations (4.5)-(4.9) become

$$\begin{aligned}W_1 &= 0,\ D\ominus_1 = 0,\ DW_1 = 0 \quad at\ z = 1\\ W_{m1} &= 0,\ D_m\ominus_{m1} = 0 \quad at\ z_m = -1.\end{aligned}$$

And at the interface(i.e $z = 1$)

$$W_1 = \frac{\zeta}{\zeta \varepsilon_T} W_{m1}, \; \ominus_1 = \frac{\varepsilon_T}{\zeta^3} \ominus_{m1}, \; D\ominus_1 = \frac{1}{\zeta^2} D_m \ominus_{m1}$$

$$D^3 W_1 - \eta D^2 W_1 = \frac{-\zeta^2}{\varepsilon_T Da \xi} D_m W_{m1}$$

$$D^2 W_1 - \frac{\beta \zeta}{\sqrt{Da\xi}} DW_1 = \frac{-\beta \zeta}{\varepsilon_T \sqrt{Da\xi}} D_m W_{m1}$$

The general solutions of equations (5.7) and (5.9) are respectively given by

$$W_1 = [C_1 + C_2 z + C_3 z^2 + C_4 e^{\eta z}]$$
$$W_{m1} = [C_5 + C_6 z_m]$$

where

$$C_1 = \left( \frac{C_2}{\varepsilon_T \xi} - \frac{\zeta^2 C_4}{\varepsilon_T \xi} \right), \quad C_2 = \left( \frac{2\xi \varepsilon_T}{\zeta^2} - \frac{C_1}{2\xi} - \frac{e^{\eta} C_4}{\zeta^2} \right),$$
$$C_3 = \frac{b_{10} + b_9 C_6}{b_4}, \qquad C_4 = \frac{b_6 \varepsilon_T \zeta - \varepsilon_T \zeta C_3 + C_3}{\xi C_1},$$
$$C_5 = \frac{C_1}{2\zeta(1+2\xi)} + C_6, \quad b_1 = \left( \frac{2\zeta^2 \sqrt{Da}}{2\xi} + \beta \zeta^3 \right),$$
$$b_2 = \left( \eta^2 \zeta^2 \sqrt{Da\xi} - \beta \zeta^3 \eta \right) - \beta \zeta^3 \left( \sqrt{Da\xi} - e^{\eta} \right),$$
$$b_3 = \left( \Delta_2 \sqrt{Da\xi} - \frac{\beta \zeta^3}{\varepsilon_T \zeta} \right), b_4 = \left( \frac{\varepsilon_T \beta \zeta^3}{6\eta \zeta} - \frac{\beta \zeta^3 \sqrt{Da\xi}}{\varepsilon_T \zeta} \right),$$
$$b_5 = (\eta - 1)e^{\eta} + \sqrt{Da\xi}, \; b_6 = \left( \frac{2\varepsilon_T}{6\eta \zeta} - \frac{\sqrt{Da\xi}}{\varepsilon_T \zeta} \right),$$
$$b_7 = \left( b_1 b_3 - \frac{b_2}{\varepsilon_T \zeta} \right), \quad b_8 = \left( b_3 b_5 - \frac{b_2}{\varepsilon_T \zeta} \right),$$
$$b_9 = (b_4 b_5 + 2 b_7 b_6), \quad b_{10} = \frac{b_1 b_7 - b_8 b_6}{b_1 b_7 - \frac{b_4}{\varepsilon_T \zeta}}.$$

Equations (5.8) and (5.10) involving $D^2\ominus_1$ and $D_m^2\ominus_{m1}$ provides the condition

$$\int_0^1 f(z) W_1 dz + \frac{\chi}{\zeta^2} \int_{-1}^0 g(z_m) W_{m1} dz = -\frac{\varepsilon_T}{\zeta} - \frac{\chi}{\zeta^2} \tag{5.11}$$

The expressions for $W_1$ and $W_{m1}$ are back substituted into equation (5.11) and integrated to yield an expression for the critical Marngoni number $M_c$, which is given by

$$M_c = \frac{-\left(\frac{\varepsilon_T}{\zeta} + \frac{\chi}{\zeta^2}\right)\left(\frac{Da\varepsilon_T^2}{\zeta^4}\right)}{(\delta_1 C_1 + \delta_2 C_2 + \delta_3 C_3 + \delta_4 C_4 + \delta_5) + \frac{\chi}{\zeta^2}(-C_5 + \delta_6 C_6 - \delta_3 \delta_7)}$$

where

$$\delta_1 = \left( \frac{4Ns}{Pe} + 1 \right), \quad \delta_2 = \left( \frac{4\zeta}{Pe} + \frac{4\zeta^3}{Pe} \right),$$
$$\delta_3 = \left[ \frac{2}{3Pe} + \frac{Pe+2}{1-e^{Pe}} \left( \frac{e^{Pe}}{Pe} - \frac{2\left(1-e^{Pe}\right)}{Pe^3} \right) \right],$$
$$\delta_4 = \left[ \frac{6}{\eta Pe} + \frac{\chi + \zeta}{1 - 3e^{Pe}} \right], \quad \delta_5 = -\frac{\varepsilon_T}{6\eta\zeta} \left[ \frac{e^{Pe}}{Pe} - \frac{6(e^{Pe}-1)}{Pe^4} \right],$$
$$\delta_6 = \left[ \frac{Pe_m + 2}{1 - e^{-Pe_m}} \left( \frac{-e^{-Pe_m}}{Pe_m} - \frac{e^{-Pe_m} - 1}{Pe_m^2} \right) \right],$$
$$\delta_7 = \left[ \frac{2}{3Pe_m} + \frac{e^{-Pe_m}}{Pe_m} + \frac{2e^{-Pe}}{Pe_m^2} + \frac{2(e^{-Pe_m} - 1)}{Pe_m^3} \right].$$

## 6. Results and Discussion

The initiation of Marangoni convection in the presence of a vertical through flow is considered in a process consisting of a liquid surface overlaid by anisotropic porous layer.

### 6.1 Depth ratio $\zeta \gg 1$

This is the case with a pure zone1 layer and the system's stability characteristic is measured by Marangoni number when $Pe = 0$, the known exact value $M = 48$ (Nield [19]) is obtained. **Figure 2** is a plot of $M$ as a function $Pe$. The following conclusions can be drawn from this figure:

(i) For upward throughflow $(Pe > 0)$ an increase in $Pe$ is to increase $M$, and thus upward throughflow makes the system more stable.

(ii) For downward throughflow $(Pe > 0)$ an increase in $Pe$ is to decrease $M$ initially, and a further increase in $Pe$ increases $M$. Thus a weak downward throughflow destabilize.

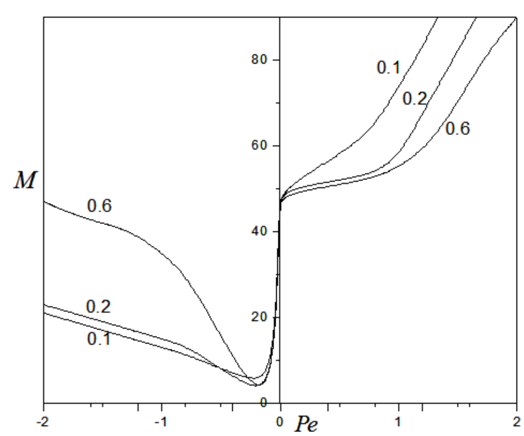


**Figure 2.** $M$ versus $Pe$ for different values of $Pr$ for a case of single fluid layer $(\zeta \ggg 1)$

### 6.2 Depth ratio $\zeta = 0.1$

The stability of the system is characterized by $M_c$. **Figure 3** exhibit plots of $M_c$ as a function of $Pe_m$ respectively for isotropic porous layer ($\chi = 1 = \xi$) and anisotropic porous layer ($\chi = 0.5 = \xi$). The results are presented for three different values of Prandtl number $Pr = 0.1, 0.5$ and 1.

From **Figure 3** it is seen that for all values of $Pr$ for the both case of isotropic and anisotropic porous layer stabilizes the system for upward throughflow and the system is destabilizing for downward throughflow when $-1.2 \leq Pe_m \leq 0$ for all three values of $Pr$ for the isotropic case and for other values of $Pe_m$ the system is stabilizing. But in the case of anisotropic the system is destabilizing $-0.9 \leq Pe_m \leq 0$ for Prandtl numbers $Pr = 0.1, 0.2$ and $-5.2 \leq Pe_m \leq 0$ for $Pr = 0.6$, respectively and for higher values of $Pe_m$ the system is stabilizing.

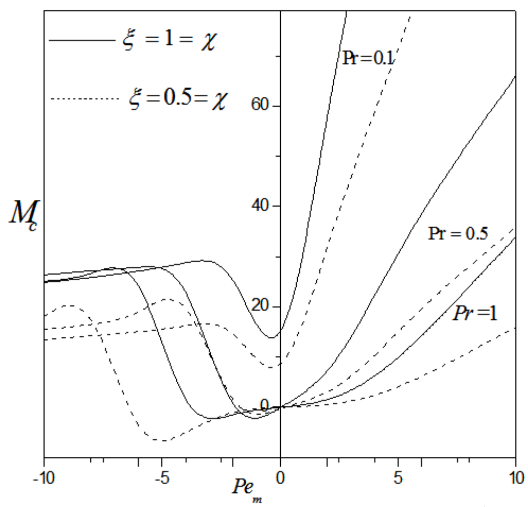


**Figure 3.** $M_c$ versus $Pe$ for different values of $\zeta = 0.1$

### 6.3 Depth ratio $\zeta = 0.2$

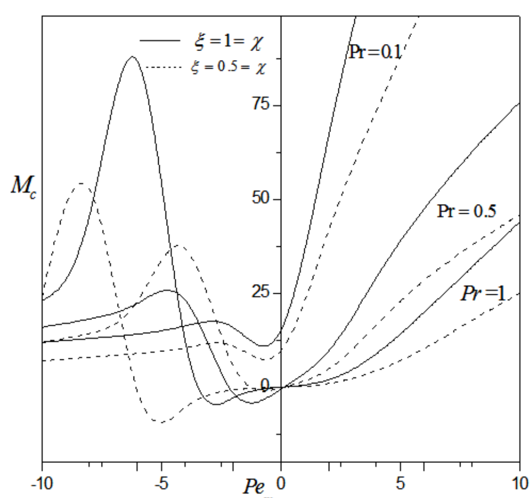


**Figure 4.** $M_c$ versus $Pe$ for different values of $Pr$ with $\zeta = 0.2$

**Figure 4** depicts plots of $M_c$ as a function of $Pe_m$ respectively for isotropic porous layer $\chi = 1 = \xi$ and anisotropic porous layer $\chi = 0.5 = \xi$. The results are presented for three values of Prandtl number $Pr = 0.1, 0.5$ and 1. From **Figure 4** it is seen that for all values of $Pr$ for the both case of isotropic and anisotropic porous layer stabilizes the system for upward throughflow and the system is stabilizing for downward throughflow when $-2.5 \leq Pe_m \leq -0.5$ for $Pr = 0.1$, when $-4 \leq Pe_m \leq -0.80$ and $-2.8 \leq Pe_m \leq 0$ for $Pr = 0.5$ and when $-5.8 \leq Pe_m \leq -3.8$ for $Pr = 1$ respectively for the isotropic case. But the system is stabilizing for downward throughflow when $-2.5 \leq Pe_m \leq -0.5$ for $Pr = 0.1$, when $-8 \leq Pe_m \leq -5$ and $-2.8 \leq Pe_m \leq 0$ for $Pr = 0.5$ and when $-4.5 \leq Pe_m \leq -2.5$ for $Pr = 1$ respectively for the anisotropic case.

### 6.4 Depth ratio $\zeta = 0.5$

**Figure 5** depicts plots of $M_c$ as a function of $Pe_m$ respectively for isotropic porous layer $\chi = 1 = \xi$ and anisotropic porous layer $\chi = 0.5 = \xi$. The results are presented for three values of Prandtl number $Pr = 0.1, 0.5$ and 1. From **Figure 5** it is seen that for all values of $Pr$ for the both case of isotropic and anisotropic porous layer stabilizes the system for upward throughflow and the system is stabilizing for downward throughflow when $-2.5 \leq Pe_m \leq -1.5$ for $Pr = 0.1$, when $-3.5 \leq Pe_m \leq -1.8$ for $Pr = 0.5$ and when $-7.5 \leq Pe_m \leq -3.5$ for $Pr = 1$ respectively for the isotropic case. But the system is stabilizing for downward throughflow when $-2.5 \leq Pe_m \leq -0.5$ for $Pr = 0.1$, when $-8 \leq Pe_m \leq -5$ and $-2.8 \leq Pe_m \leq 0$ for $Pr = 0.5$ and when $-5.5 \leq Pe_m \leq -8.5$ for $Pr = 1$ respectively for the anisotropic case.

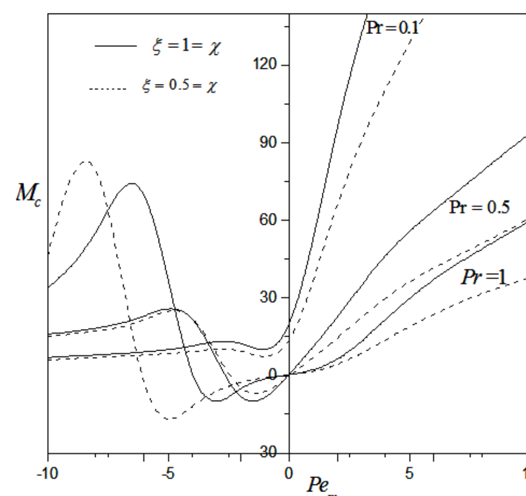


**Figure 5.** Critical Marangoni number versus $Pe$ for different values of $Pr$ with $\zeta = 0.5$

### 6.5 Depth ratio $\zeta = 1$

**Figure 6** depicts plots of $M_c$ as a function of $Pe_m$ respectively for isotropic porous layer $\chi = 1 = \xi$ and anisotropic porous layer $\chi = 0.5 = \xi$. The results are presented for three values of Prandtl number $Pr = 0.1, 0.5$ and 1. From **Figure 6** it is seen that for all values of $Pr$ for the both case of isotropic and anisotropic porous layer stabilizes the system for upward throughflow and the system is destabilizing for downward throughflow for $Pr = 0.1$, and the system is stabilizing when $-2.5 \le Pe_m \le 0$ for $Pr = 0.5$ and when $-6.5 \le Pe_m \le -2.5$ for $Pr = 1$ respectively for the isotropic case. But the system is destabilizing for downward throughflow for $Pr = 0.1$ and system is stabilizing when $-2.5 \le Pe_m \le 0$ for $Pr = 0.5$ and when $-8.5 \le Pe_m \le -5$ for $Pr = 1$ respectively for the anisotropic case.

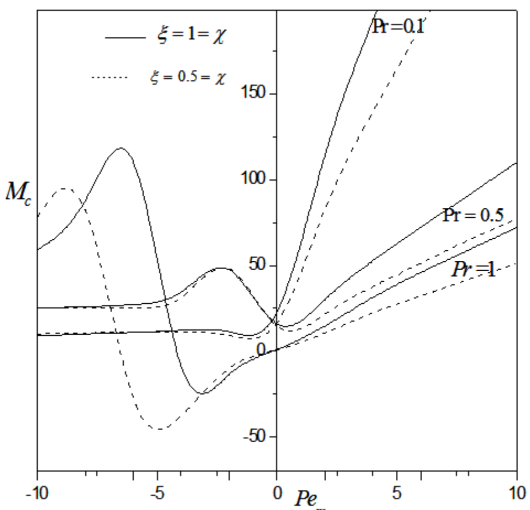


**Figure 6.** Critical Marangoni number versus $Pe$ for different values of $Pr$ with $\zeta = 1$

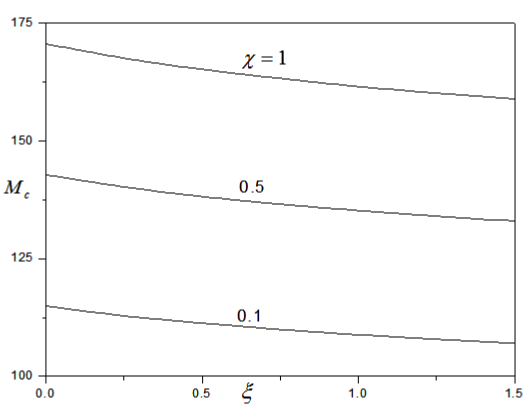


**Figure 7.** $Mc$ versus $\xi$ for different values of $\chi$ with $Pr = 1$ and $\zeta = 1$

The effect of $\xi$ and $\chi$ on the onset of convection is emphasized by depicting the variation of $M_c$ and over a range of $\xi$ for different values of $\chi$ in **Figure 7** for a fixed value of $Pr = 1$, $\zeta = 1$. It is observed that $M_c$ increases with the decreasing $\xi$. It mechanically means the conductive solution becomes more stable in the porous medium.

## 7. Conclusions

In an anisotropic porous layer underlined by a fluid layer, an exact analysis is made to study the influence of throughflow on the onset of Marangoni convection. It is observed from the above analysis that the stability characteristics of the configuration are crucially dependent on

(i) throughflow direction

(ii) depth ratio $\zeta$

(iii) mechanical anisotropy parameter $\xi$

(iv) thermal anisotropy parameter $\chi$.

Therefore, convective instability resulting either in a porous layer or in a fluid layer by adjusting the $\zeta$ or $Pe$ or $\xi$ or $\chi$ by considering all the effects together, since both the stabilizing and the destabilizing factors can be increased more in the combined porous and fluid layer system than in the combined porous and fluid layer system.

## References

[1] K. Vafai, *Handbook of Porous Media*, Taylor/CRC Press, Francis, London/Boca Raton, FL, 2005.

[2] D. A. Nield and A. Bejan, *Convection in Porous Media*, Second ed. Springer-Verlag, New York, 2006.

[3] D. A. Nield and A. Bejan, *Convection in Porous Media*, Springer, New York, 2013.

[4] J. B. Grotberg, and D. P. Gaver, A synopsis of surfactant spreading research, *Journal of Colloid and Interface Science.* 178(1996), 377–378.

[5] D. P. Gaver, J. B. Grotberg, Droplet Spreading on a Thin Viscous Film, *J Fluid Mech.* 235(1992), 399–414.

[6] D. P. Gaver and J. B. Grotberg, The dynamics of a localized surfactant on a thin film, *J. Fluid. Mech.* (1990).

[7] A. B. Afsar-Siddiqui, P. F. Luckham and O. K. Matar, The spreading of surfactant solutions on thin liquid films, *Advances in Colloid and interface science.* 03(2003), 1–8.

[8] J. B. Grotberg, Respiratory fluid mechanics and transport processes, *Annu. Rev. Biomed. Eng.* 3(2001), 421–457.

[9] D. Halpern, O. E. Jensen and J. B. Grotberg, A theoretical study of surfactant and liquid delivery into the lung, *J. Appl. Physiol.* 85(1998), 333–352.

[10] C. D. Bertram and D. P. Gaver, Biofluid Mechanics of the Pulmonary System, *Ann. Biomed. Eng.* 33(2005), 1681–1688.

[11] F. Chen, Throughflow effects on convective instability in superposed fluid and porous Layers, *J. Fluid. Mech.* 231(1990), 113–133.

[12] A. Khalili, I. S. Shivakumara and S. P. Suma, Convective instability in superposed fluid and porous layers with vertical throughflow, *Transp. Porous Med.* 51(2003), 1–18.

[13] S. P. Suma, Y. H. Gangadharaiah, R. Indira and I. S. Shivakumara, Throughflow effects on penetrative convection

in superposed fluid and porous layers, *Transp. Porous Med.* 95(2012), 91–110.

[14] I. S. Shivakumara, S. P. Suma, R. Indira and Y. H. Gangadharaiah, Effect of internal heat generation on the onset of Marangoni convection in a fluid layer overlying a layer of an anisotropic porous medium, *Transp. Porous Med.* 92(2012), 727–743.

[15] I.S. Shivakumara, M. Venkatachalappa and S.P. Suma, Exact analysis of Marangoni convection with throughflow, *Acta Mech*. 136(1999), 109–117.

[16] S. Saravanan and T. Sivakumar, Exact solution of Marangoni convection in a binary fluid with throughflow and Soret effect, *Applied Mathematical Modelling*. 33(2009), 3674–3681.

[17] I. S. Shivakumara, Jinho Lee and K. B. Chavaraddi, Onset surface tension convection in a fluid layer overlying a layer of an anisotropic porous medium, *Int. J. Heat Mass Transf.* 54(2011), 994–1001.

[18] G. S. Beavers and D. D. Joseph, Boundary conditions at a naturally permeable wall, *J. Fluid Mech.* 30(1967), 197–207.

[19] D. A. Nield, The onset of transient convective instability, *J. Fluid Mech.* 71(1975), 441–454.

⋆⋆⋆⋆⋆⋆⋆⋆⋆
ISSN(P):2319 − 3786
Malaya Journal of Matematik
ISSN(O):2321 − 5666
⋆⋆⋆⋆⋆⋆⋆⋆⋆